RXTE observations of A1744–361: correlated spectral and timing behavior

Sudip Bhattacharyya[1,2], Tod E. Strohmayer[2], Jean H. Swank[2], and Craig B. Markwardt[1,2]

ABSTRACT

We analyze Rossi X–ray Timing Explorer (*RXTE*) Proportional Counter Array (PCA) data of the transient low mass X–ray binary (LMXB) system A1744–361. We explore the X–ray intensity and spectral evolution of the source, perform timing analysis, and find that A1744–361 is a weak LMXB, that shows 'atoll' behavior at high intensity states. The color-color diagram indicates that this LMXB was observed in a low intensity spectrally hard (low-hard) state and in a high intensity 'banana' state. The low-hard state shows a horizontal pattern in the color-color diagram, and the previously reported 'dipper QPO' appears only during this state. We also perform energy spectral analyses, and report the first detection of broad iron emission line and iron absorption edge from A1744–361.

Subject headings: methods: data analysis — stars: neutron — techniques: miscellaneous — techniques: spectroscopic — X-rays: binaries — X-rays: individual (A1744–361)

1. Introduction

The transient low mass X–ray binary (LMXB) A1744–361 was discovered by Ariel V in 1976, when it was in outburst (Davison et al. 1976; Carpenter et al. 1977). Since then four more outbursts have been observed from this source in the years 1989, 2003, 2004 and 2005. Bhattacharyya et al. (2006) found an unambiguous thermonuclear X–ray burst from the 2005 *RXTE* PCA data of this source, which confirmed the suggestion of Emelyanov et al. (2001) that this source harbors a neutron star. This burst also showed millisecond period brightness oscillations during the intensity rise (with the frequency ~ 530 Hz; Bhattacharyya

---

[1]Department of Astronomy, University of Maryland at College Park, College Park, MD 20742-2421

[2]X-ray Astrophysics Lab, Exploration of the Universe Division, NASA's Goddard Space Flight Center, Greenbelt, MD 20771; sudip@milkyway.gsfc.nasa.gov, stroh@clarence.gsfc.nasa.gov, swank@milkyway.gsfc.nasa.gov, craigm@milkyway.gsfc.nasa.gov

et al. 2006), which gave the spin frequency of the neutron star (~ 530 Hz). This is because, these oscillations are produced by an asymmetric brightness pattern on the stellar surface that is modulated by rotation of the star (Strohmayer et al. 1996; Chakrabarty et al. 2003; Strohmayer & Bildsten 2006). Bhattacharyya et al. (2006) also found energy dependent dips in the 2003 PCA data, which established that this source is a dipping LMXB (dipper). Such LMXBs exhibit modulation of soft X-ray intensity with the binary orbital period (which gave the orbital period ~ 97 min of A1744–361; Bhattacharyya et al. 2006). This modulation is believed to be caused by structures above the accretion disk (White & Swank 1982). This is possible only if the dippers are high inclination systems, so that the line of sight passes through these structures. Therefore, dippers provide an opportunity to constrain the properties of the upper layers of accretion disks (and the photoionized plasma above them; Jimenez-Garate et al. 2003) in LMXBs. Moreover, recently spectral lines have been discovered from several dippers, such as EXO 0748-67 (Cottam et al. 2001), XB 1916–053 (Boirin et al. 2004), X 1624–490 (Parmar et al. 2002), etc. This shows that A1744–361 might be a promising source to search for these features, which could be useful to understand various X–ray emitting and absorbing components of LMXBs.

It is also important to determine the broad spectral and timing category (e.g., Z, atoll, weak LMXB, etc.; see, for example, van der Klis 2004; Kuulkers et al. 1997; Wijnands et al. 1998; Bhattacharyya 2006) of A1744–361 in order to understand the nature of this source. Z sources are the most luminous LMXBs and trace 'Z'-like curves (with three branches: horizontal, normal and flaring) in the color-color diagram. The ordinary atoll sources have luminosities in the range $\sim 0.01 - 0.2 L_{\mathrm{Edd}}$ (L_{Edd} is the Eddington luminosity), and trace 'C'-like curves (with two branches: low intensity 'island' and high intensity 'banana'; van der Klis 2004). The various portions of these curves (combined with the correlated timing features) indicate different source states (van der Klis 2004). Recently, a low intensity spectrally hard (low-hard) state has been observed from several atoll sources. Because of its horizontal branch like pattern in the color-color diagram, some authors (Muno, Remillard, & Chakrabarty 2002 (hereafter MRC); Gierliński & Done 2002) suggested that this state might be to some extent similar to the horizontal branch state of Z sources. Such a picture, if true, favors at least partial unification of Z and atoll sources. However, this horizontal branch of atoll sources occurs at a much lower luminosity, much harder spectral state, and with a much longer time scale (compared to those of Z sources; MRC), and hence we call this state 'atoll horizontal branch' (AHB). Here we note that AHB might actually be the known extreme island state (EIS; van der Klis 2004) of atoll sources, and detailed study of the low intensity states of the atoll sources is necessary to resolve this. We also note that there is another category of LMXBs (known as weak LMXB; luminosity $\lesssim 0.01 L_{\mathrm{Edd}}$), which comprises the faint burst sources, the low-luminosity transients, etc. Many of these sources

appear to be low-luminosity atoll sources (van der Klis 2004), and show timing properties similar to those of atoll sources.

In § 2, we calculate the color-color diagram and perform timing analysis to show that A1744–361 is a weak LMXB, that exhibits atoll behavior at high luminosities. We also suggest that the previously discovered low frequency dipper QPO (Bhattacharyya et al. 2006; Jonker, van der Klis & Wijnands 1999) is connected to the low-hard state of the source. In § 3, we describe the first detection of broad iron emission line and iron absorption edge from the energy spectra of A1744–361, and in § 4 we discuss our results.

2. Color-Color Diagram and Timing Analysis

The transient source A1744–361 was observed with *RXTE* during three outbursts. The duration (year, RXTE proposal number, RXTE observation duration) of these outbursts were ~ 2 months (2003, P80431, ~ 39 ks), ~ 20 days (2004, P90058, ~ 2 ks), and ~ 40 days (2005, P91050, ~ 15 ks). The time intervals of the pointed observations with *RXTE* are shown in Fig. 1. Here each interval is during an outburst, and contains several observations. This figure shows that the first (2003) outburst was the strongest and the longest, and it had two peaks. The 2005 outburst was also strong, but the 2004 outburst was weak and gives the opportunity to understand the source in a low-hard state (see later). The pointed observations were made near the first peak of the 2003 outburst, and near the peaks of the other two outbursts. We have computed a color-color diagram (CD; Fig. 2) using the *RXTE* PCA (from only the top Xenon layers to increase signal to noise) pointed observations. These data are from the same gain epoch (epoch 5), and hence the gains of the Proportional Counter Units (PCUs) are almost the same. This ensures minimal shifting of the source track in the CD due to the differences of the energy boundaries. The PCUs 0, 2 and 3 were reliably on during most of these observations, and we have used the data from these PCUs to calculate most of the CD. However, for a few ObsIDs we have used data from other PCU combinations. For these ObsIDs, we choose the PCA channel ranges carefully, so that the energy boundaries are similar to those for other ObsIDs. We have defined soft and hard colors (used in the CD; Fig. 2) as the ratio of the background-subtracted counts approximately in the $(3.5 - 5.1)/(2.2 - 3.5)$ and $(8.5 - 17.8)/(5.1 - 8.5)$ keV energy bands respectively. We have also calculated a hardness-intensity diagram (HID; Fig. 2) using these data with the background-subtracted intensity in the energy range $\sim 2.2 - 17.8$ keV. These definitions are close to the definitions used by MRC, and will facilitate the comparison of our results with those of these authors. Here we note that we have used 'FTOOLS' command 'pcabackest' for estimating the backgrounds. This is because the source was always $> 10 - 100$ times

brighter than the galactic ridge, and hence the ridge contribution (see § 3) to the colors is not significant.

From the CD and the HID, it is clear that A1744–361 was observed in two distinctly different states: a low intensity spectrally hard (low-hard) state in 2004 and a high intensity state in 2003 and 2005. In order to explore the nature of A1744–361, first we have calculated the typical X–ray fluxes from this source in these two states by fitting spectra with models. The $2 - 20$ keV fluxes are $\sim 4.3 \times 10^{-10}$ and $\sim 3.2 \times 10^{-9}$ ergs cm^{-2} s^{-1} respectively. The peak $2 - 20$ keV flux during a non-photospheric-radius-expansion thermonuclear X–ray burst from this source was 1.9×10^{-8} ergs cm^{-2} s^{-1} (Bhattacharyya et al. 2006), which implies that the low intensity state luminosity $L_{\mathrm{low}}/L_{\mathrm{Edd}} \lesssim 0.02$ and the high intensity state luminosity $L_{\mathrm{high}}/L_{\mathrm{Edd}} \lesssim 0.17$. Here, L_{Edd} is the Eddington luminosity. The luminosities of the high intensity state are consistent with those of atoll sources, while the luminosities of the low intensity state are consistent with those of weak LMXBs or atoll sources (van der Klis 2004). Therefore, as the source remains in a very low intensity (quiescent) state most of the time and rarely exhibits an outburst (see Fig. 1), it is likely that A1744–361 is a weak LMXB, that shows atoll behavior at high intensity states. Here we note that the typical luminosities of Z sources are close to the Eddington luminosity (van der Klis 2004), and hence much higher than the luminosity of A1744–361. So it is not likely that A1744–361 is a Z source.

In order to more definitively show that this source is not a Z source, next we have compared our CD (Fig. 2) with that of MRC. Fig. 1 of MRC shows that the flaring branches (FBs) of Z sources have hard colors close to 0.2 (except for GX 17+2). As the hard colors of A1744–361 in the high intensity state are close to 0.3, this indicates that if this source is a Z source, it was not in an FB state during the 2003 and 2005 observations. Besides, during the 2003 observations the source showed flares, which are not usual for the other two states (normal branch and horizontal branch) of Z sources. Apart from this, the hard colors of A1744–361 in the low intensity state are close to $5.5 - 6$. Z sources normally do not show such high values of hard colors (see Fig. 1 of MRC). Therefore, we conclude that A1744–361 is not a Z source.

Fig. 1 of MRC shows that the hard colors of atoll sources are always around or greater than 0.3 (except for GX 13+1). This, and especially the observed hard colors of the banana branches of atoll sources (see MRC) strongly indicate that A1744–361 was in the banana branch during 2003 and 2005 observations (high intensity states; see Fig. 2). This supports our earlier conjecture that A1744–361 shows atoll behavior at high intensity states. Here we note that during the first observation of 2005 (ObsID 91050-05-01-00), the source was spectrally slightly harder and less intense (*square* symbols in Fig. 2), which might be an

indication of transition between banana and island states (van der Klis 2004). We also note that this observation registers the only thermonuclear X–ray burst seen from this source (Bhattacharyya et al 2006; see also Fig. 2).

The CD (Fig. 2) shows that A1744–361 traced a horizontal pattern at high hard color values in 2004. This is likely to indicate the AHB state (see § 1) of the source, because its intensity was very low, it was spectrally very hard, and it followed a horizontal track in the CD. But the small amount of observation does not allow us to determine the duration of this state. However, the time separation between the two ObsIDs (90058-04-01-00 & 90058-04-02-00) in this state was ∼ 40 hrs., which may indicate that at least during this time period the source was in this low-hard state. We also note that A1744–361 was not detected with hard colors in the range ∼ 0.37 − 0.5, and it seems that the future observation of these hard colors will be indicative of the island state of the source (van der Klis 2004).

As a source state is characterized by its timing properties in addition to the position of the source on the CD, we have computed and fitted the power spectra of A1744–361 (Table 1). We have found that the high frequency power spectra of all data segments are featureless, and show only white noise (but see Bhattacharyya et al. 2006 for the description of a possible kHz QPO). Therefore, in this paper we have computed and fitted the low frequency (up to ∼ 100 Hz) power spectra of the data of four representative portions of the CD (Fig. 3). In these calculations we have used the data from all the available PCUs from event mode files, and divided the data into 250 s segments. Then we have binned (of 1/256 s size) each segment, and performed fast Fourier transform. An average of all these transforms from a data set gave the power spectrum. This spectrum has been binned geometrically in order to increase the signal to noise. Fig. 3 shows these spectra (from four data sets), the best fit models, and the positions of the corresponding data segments on the CD. The best fit parameter values are given in Table 1. The power spectrum of the low intensity AHB state (2004 data) of A1744–361 can be sufficiently modeled with a constant (describing the white noise) and a Lorentzian (describing the dipper QPO; Bhattacharyya et al. 2006). The centroid frequency and the rms of the Lorentzian do not significantly depend on photon energies (within error bars), which is consistent with the 'dipper QPO' interpretation of this feature (Jonker et al. 1999). The power spectra of all the high intensity states (2003 and 2005 data) of the source are well fitted with a constant and a power-law. The power-law describes the 'very low frequency noise' (VLFN; van der Klis 2004; Boirin et al. 2000; Berger, & van der Klis 1998; Agrawal & Bhattacharyya 2003), which strongly indicates that A1744–361 was on the banana branch in 2003 and 2005. However, during the first observation of 2005 (ObsID 91050-05-01-00), the strength of the VLFN was significantly less than that during the other observations (at high source intensity; see Table 1 and Fig. 3). This supports the guess (made earlier in this section) that during this 2005 observation, the source was in a

transition state (between banana and island; van der Klis 2004).

3. Spectral Analysis

A CD gives an idea about the spectral evolution of the source. But to fully understand the spectral properties of A1744–361, a detailed spectral analysis is essential. However, before describing such an analysis, we note that *RXTE* PCA registered excess X–ray emission from the galactic ridge during the pointed observations of the source. This is because the location of A1744–361 is in the galactic ridge (galactic latitude $\approx$ $-4°.2$), and the FWHM spatial resolution of the PCA is 1° (Valinia & Marshall 1998). Therefore, we need to take this emission into account during each spectral fitting, especially if we are interested in iron features in the spectrum (as the unresolved excess emission contains an iron emission line (at $\sim$ 6.7 keV); Koyama et al. 1986). But, the 'pcabackest' command (for background calculation) of 'FTOOLS' does not include the galactic ridge contribution (Jahoda et al. 2005). We should, therefore, model the galactic ridge spectrum at the position of A1744–361 (when the source is not in outburst) and use this model (with the parameters frozen to the best fit values) in addition to the other model components to describe the source spectra.

Hence, as the first step of our spectral analysis, we have fitted $\sim$ 1 ks of 'pcabackest' background subtracted *RXTE* PCA spectrum from the galactic ridge (from the position of quiescent A1744–361) with the absorbed 'Raymond-Smith' plus power-law model (*wabs*(raymond+powerlaw)*; Valinia & Marshall 1998). The best fit parameters are given in Table 2. We have used this model (with these best fit parameter values) as a model component for all the source spectral analyses. Next, we have chosen a high intensity source data segment (ObsID 80431-01-02-02) in order to find out typical spectral properties of A1744–361 during high intensity states. We have fitted (after 'pcabackest' background subtraction) the corresponding spectrum with various *XSPEC* models (see Table 3). The model that gives a reasonable χ^2/dof value, contains an absorbed Comptonization (*compST* in *XSPEC*) plus blackbody (*bbodyrad* in *XSPEC*) as the continuum, a broad emission line (*gauss* in *XSPEC*) and an absorption edge (*edge* in *XSPEC*). Here we note that we have fixed the lower limit of the hydrogen column density (N_H) to 0.1×10^{22} cm^{-2}, so that this parameter does not wander to an unphysically small value (NASA's HEASARC nH tool gives $N_H \approx 0.3 \times 10^{22}$ cm^{-2} in the source direction). We have also fixed the upper limit of the width (σ_G; see Table 4) of the Gaussian emission line to 1.0 keV during spectral fitting (as D' Aí et al. 2006 did), so that this line does not become unphysically broad. Moreover, as the lowest centroid energy of broad emission lines found by Asai et al. (2000) was 5.9 keV, we have chosen this energy to be the lower limit of our Gaussian line centroid energy. From Table 3, we find that

both the emission line and the absorption edge of the best fit model are significantly detected (see Fig. 4). With this knowledge, we have, then, fitted the spectra of three additional data segments (one high intensity and two low intensity). Table 4 shows the best fit parameter values from these spectral analyses, as well as from the fitting of the spectrum of Table 3. The emission line and the absorption edge significantly appear in both the high intensity spectra. However, we do not find the blackbody component and the emission line in the low intensity spectra, although the absorption edge component is significantly present. The centroid energy of the emission line ($\sim$ 6 keV) and the threshold energy of the absorption edge ($\sim$ 8 keV) indicate that these are iron features (Asai et al. 2000; D' Aí et al. 2006). From our results, and as the galactic ridge spectrum is separately modeled, we conclude that the broad emission line and the absorption edge originated from A1744–361.

4. Discussion

In this paper, we have reported the correlated spectral and timing behavior of the LMXB A1744–361 for the first time, as well as the first discovery of iron features (broad emission line and absorption edge) in the energy spectra from this source. We have estimated the luminosity range (in the unit of Eddington luminosity) of A1744–361, calculated the color-color diagram, hardness-intensity diagram and power spectra of this source, and found that A1744–361 is a weak LMXB, which shows atoll behavior during outbursts. The source was observed at low luminosity during the weak outburst in 2004, and at high luminosity during the strong outbursts in 2003 and 2005. During the 2004 outburst, A1744–361 was in the low-hard state, but there were not enough pointed observations to determine whether the source was in such a state during the rise or decay of 2003 and 2005 outbursts. Our analysis suggests that the dipper QPO (found by Bhattacharyya et al. 2006) is connected to the low-hard state (AHB; see Figs. 2 and 3) of the source. This is consistent with the finding of such a QPO from the LMXB 4U 1746–37 only during the low-hard state (Jonker et al. 2000). Also note that the dipper QPO from the LMXB EXO 0748–676 was observed during the low intensity state, but not during the high intensity state (Homan et al. 1999). The energy dependent dips of A1744–361 (discovered by Bhattacharyya et al. 2006) were observed only during the high intensity states of the source (see Fig. 2). This indicates that for A1744–361 the dips are correlated with the source states.

Spectral analyses show that the continuum part of the source spectra are well described by a Comptonization plus blackbody (high intensity) or by a Comptonization (low intensity). The Comptonization component might originate from an extended corona, while the origin of the blackbody might be the neutron star surface and/or the inner accretion disk (D' Aí

et al. 2006; White et al. 1986; Church & Balucińska-Church 2004). However, we note that some other model components (such as a bremsstrahlung, or a cutoff-powerlaw) instead of Comptonization also give reasonable fits for most of the cases. Nevertheless, we have used a simple Comptonization model for all our analyses, because a Comptonization component was likely to be present in the spectrum (D' Aí et al. 2006), and with the first discovery of a broad emission line and an absorption edge in the A1744–361 spectra, we have primarily focused on these features.

The threshold energies of the absorption edge are within the range $7 - 9$ keV (Table 4), and hence are consistent with those expected from ionized iron (D' Aí et al. 2006). The emission line is broad, and such broad iron lines (near 6 keV) are observed from many LMXBs, including dippers (Asai et al. 2000). These lines may be broadened by either Doppler effects due to Keplerian motion in the inner accretion disk, or Compton scattering in disk corona (Asai et al. 2000). Analysis of high resolution spectra can likely determine the source of this broadening by measuring the detailed structure of these lines. If the Doppler effect is determined to be the real cause, then the shapes and widths of these lines may be used to constrain the inner edge radius of the disk, as well as the Keplerian speed at that radius. The former can give an upper limit of the neutron star radius (as the disk inner edge radius must be greater than or equal to the stellar radius), while both quantities may be utilized to constrain the stellar mass. Note that the constraints on neutron star mass and radius can be useful to understand the nature of the high density cold matter at the stellar core, which is a fundamental problem of physics (e.g., Lattimer & Prakash 2001; Bhattacharyya et al. 2005). The centroid energy of the broad iron emission line observed from A1744–361 is less than 6.4 keV, which could be due to unresolved iron absorption lines near ~ 7 keV (Parmar et al. 2002). This suggests that A1744–361 might show spectral absorption lines when observed with higher spectral resolution missions (e.g., *Chandra*, *XMM-Newton* and *Suzaku*).

REFERENCES

Agrawal, V. K., & Bhattacharyya, S. 2003, A&A, 398, 223.

Asai, K., Dotani, T., Nagase, F., & Mitsuda, K. 2000, ApJSS, 131, 571.

Berger, M., & van der Klis, M. 1998, A&A, 340, 143.

Bhattacharyya, S. 2006 (astro-ph/0605510).

Bhattacharyya, S., Strohmayer, T. E., Markwardt, C. B., & Swank, J. H. 2006, ApJ, 639, L31.

Bhattacharyya, S., Strohmayer, T. E., Miller, M. C., & Markwardt, C. B. 2005, ApJ, 619, 483.

Boirin, L., Barret, D., Olive, J. F., Bloser, P. F., & Grindlay, J. E. 2000, A&A, 361, 121.

Boirin, L., Parmar, A. N., Barret, D., Paltani, S., & Grindlay, J. E. 2004, A&A, 418, 1061.

Carpenter, G. F., Eyles, C. J., Skinner, G. K., Wilson, A. M., & Willmore, A. P. 1977, MNRAS, 179, 27p.

Chakrabarty, D. et al. 2003, Nature, 424, 42.

Church, M. J., & Balucińska-Church, M. 2004, MNRAS, 348, 955.

Cottam, J., Kahn, S. M., Brinkman, A. C., den Herder, J. W., & Erd, C. 2001, A&A, 365, L277.

D' Aí et al. 2006, A&A, 448, 817.

Davison, P., Burnell, J., Ives, J., Wilson, A., & Carpenter, G. 1976, IAUC, 2925.

Emelyanov, A. N., Aref'ev, V. A., Churazov, E. M., Gilfanov, M. R., & Sunyaev, R. A. 2001, Astronomy Letters, 27, 781.

Gierliński, M. & Done, C. 2002, MNRAS, 331, L47.

Homan, J., Jonker, P. G., Wijnands, R., van der Klis, M., & van Paradijs, J. 1999, ApJ, 516, L91.

Jahoda, K. et al. 2006, ApJS, 163, 401.

Jimenez-Garate, M. A., Schulz, N. S., & Marshall, H. L. 2003, ApJ, 590, 432.

Jonker, P. G. et al. 2000, ApJ, 531, 453.

Jonker, P. G., van der Klis, M., & Wijnands, R. 1999, ApJ, 511, L41.

Koyama, K., Makishima, K., Tanaka, Y., & Tsunemi, H. 1986, PASJ, 38, 121.

Kuulkers, E., van der Klis, M., Oosterbroek, T., van Paradijs, J., & Lewin, W.H.G. 1997, MNRAS, 287, 495.

Lattimer, J. M., & Prakash, M. 2001, ApJ, 550, 426.

Muno, M. P., Remillard, R. A., & Chakrabarty, D. 2002, ApJ, 568, L35 (MRC).

Parmar, A. N., Oosterbroek, T., Boirin, L., & Lumb, D. 2002, A&A, 386, 910.

Strohmayer, T. E., & Bildsten, L. 2006, in *Compact stellar X-ray Sources*, Eds. W.H.G. Lewin and M. van der Klis, (Cambridge University Press: Cambridge), (astro-ph/0301544).

Strohmayer, T. E., et al. 1996, ApJ, 469, L9.

Valinia, A., & Marshall, F. E. 1998, ApJ, 505, 134.

van der Klis, M. 2004, in *Compact stellar X-ray Sources*, Eds. W.H.G. Lewin and M. van der Klis, (Cambridge University Press: Cambridge), (astro-ph/0410551).

Wijnands, R. et al. 1998, ApJ, 493, L87.

White, N. E. et al. 1986, MNRAS, 218, 129.

White, N. E., & Swank, J. H. 1982, ApJ, 253, L61.

Table 1. Best fit parameters[a] (with 1σ error) for the low frequency (up to ~ 100 Hz) *RXTE* power spectra from A1744–361.

Reference panel no.[b]	PLN ν[c]	PLN rms[d] (%)	L_{f_0}[e] (Hz)	L_λ[f] (Hz)	L_{rms}[g] (%)	χ^2/dof
1	–	–	2.43 ± 0.13	2.68 ± 0.42	13.1 ± 0.7	22.51/18
2	-1.50 ± 0.21	2.0 ± 1.3	–	–	–	28.66/30
3	-1.00 ± 0.03	6.7 ± 0.2	–	–	–	23.26/30
4	-0.94 ± 0.02	6.5 ± 0.2	–	–	–	25.60/24

[a]Power spectra are fitted either by constant+Lorentzian, or by constant+powerlaw in the energy range $\sim 2.6 - 30$ keV.

[b]No. of the panel in Fig. 3, that shows the power spectrum and the position of the time segment in the color-color diagram.

[c]Index of power law ($\propto f^\nu$; f is frequency) noise.

[d]RMS of power law; lower limit of integration is 0.004 Hz.

[e]Centroid frequency of Lorentzian ($\propto \lambda/[(f - f_0)^2 + (\lambda/2)^2]$).

[f]Full width at half maximum (FWHM) of Lorentzian.

[g]RMS of Lorentzian.

Table 2. Best fit model[a] parameters for the $\sim 3.4 - 14$ keV galactic ridge spectrum (*RXTE* PCA) from the position of A1744–361 (when this source was not in outburst).

Model Component	Parameter	value[b]
Absorption	N_H (10^{22} cm^{-2})	$2.5^{+3.5}_{-2.5}$
Raymond-Smith	kT (keV)	$1.8^{+0.7}_{-0.3}$
Power law	Photon index	$1.4^{+0.9}_{-0.8}$

[a]*wabs(raymond+powerlaw)* model in *XSPEC*.

[b]Reduced $\chi^2 = 15.8/21$. Flux $= 2.2 \times 10^{-11}$ ergs cm^{-2} s^{-1} (3.4 $-$ 14 keV).

Table 3.   Fitting of high intensity energy spectrum (ObsID 80431-01-02-02; *RXTE* PCA) from A1744–361 with various spectral models of *XSPEC*.

Model no.	Model[a]	χ^2/dof
1	*'ridge'+wabs*compST*	$\frac{2010.0}{22} = 91.4$
2	*'ridge'+wabs*(compST+bbodyrad)*	$\frac{757.3}{20} = 37.9$[b]
3	*'ridge'+wabs*(compST+bbodyrad+gauss)*	$\frac{27.5}{17} = 1.6$
4	*'ridge'+wabs*edge*(compST+bbodyrad+gauss)*	$\frac{8.8}{15} = 0.6$[c]

[a]The *'ridge'* model is the best fit model for galactic ridge spectrum (Table 2), and the parameters are frozen to the best fit values.

[b]See Fig. 4.

[c]The probability (calculated from F-test) of the decrease of χ^2/dof by chance from the value of the previous row to the that of the current row is 2.0×10^{-4}.

Table 4. Best fit parameters (with 1σ error) for the *RXTE* PCA energy spectra[a] from A1744–361.

Model parameters	1	2	3	4
N_H[b]	$0.10^{+0.41}_{-0.00}$	$0.12^{+0.41}_{-0.02}$	$2.05^{+0.72}_{-0.73}$	$0.55^{+1.00}_{-0.45}$
E_{edge}[c]	$8.43^{+0.16}_{-0.08}$	$8.35^{+0.12}_{-0.14}$	$8.68^{+0.36}_{-0.32}$	$7.89^{+0.20}_{-0.18}$
D_{edge}[d]	$0.12^{+0.02}_{-0.03}$	$0.07^{+0.02}_{-0.02}$	$0.16^{+0.04}_{-0.04}$	$0.18^{+0.05}_{-0.05}$
T_C[e]	$3.39^{+1.63}_{-0.29}$	$4.52^{+0.28}_{-0.23}$	$4.06^{+0.78}_{-0.44}$	$3.56^{+0.37}_{-0.18}$
τ_C[f]	$9.45^{+0.05}_{-1.25}$	$7.07^{+0.04}_{-0.33}$	$11.09^{+1.32}_{-1.45}$	$13.36^{+0.93}_{-1.51}$
T_{BB}[g]	$1.31^{+0.12}_{-0.06}$	$1.28^{+0.009}_{-0.007}$	–	–
E_G[h]	$5.97^{+0.04}_{-0.04}$	$5.90^{+0.06}_{-0.0}$	–	–
σ_G[i]	$0.62^{+0.08}_{-0.09}$	$0.69^{+0.08}_{-0.15}$	–	–
EW[j]	119^{+62}_{-27}	121^{+17}_{-35}	–	–
Flux[k]	2.2×10^{-9}	2.1×10^{-9}	3.1×10^{-10}	2.9×10^{-10}
$\dfrac{\chi^2}{\text{dof}}$	$\dfrac{8.8}{15}$	$\dfrac{13.5}{11}$	$\dfrac{13.1}{20}$	$\dfrac{11.7}{20}$

[a]1: ObsID 80431-01-02-02 (*plus* symbols of panel *d* of Fig. 3); 2: ObsID 80431-01-02-04 (*plus* symbols of panel *c* of Fig. 3); 3: ObsID 90058-04-01-00 (*diamond* symbols of Fig. 2); 4: ObsID 90058-04-02-00 (*cross* symbols of Fig. 2). First two spectra (high intensity) are fitted with '*ridge*'+*wabs**edge*(*compST*+*bbodyrad*+*gauss*) model of *XSPEC* ('*ridge*' model is described in Table 3), while the last two spectra (low intensity) are fitted with '*ridge*'+*wabs**edge*compST model.

[b]Hydrogen column density (10^{22} cm^{-2}) from *wabs* model in *XSPEC*; imposed lower limit is 0.1.

[c]Threshold energy (keV) of the edge (*edge* model in *XSPEC*).

[d]Absorption depth at the threshold of the edge.

[e]Temperature (keV) of Comptonization spectrum (*compST* model in *XSPEC*).

[f]Optical depth of Comptonization spectrum.

[g]Blackbody temperature (keV) (*bbodyrad* model in *XSPEC*).

[h]Centroid energy (keV) of Gaussian emission line (*gauss* model in *XSPEC*); imposed lower limit is 5.9.

[i]Width (keV) of Gaussian emission line; imposed upper limit is 1.0.

[j]The equivalent width (eV) of Gaussian emission line.

[k]Flux in ergs cm^{-2} s^{-1} $(3.4 - 14$ keV).
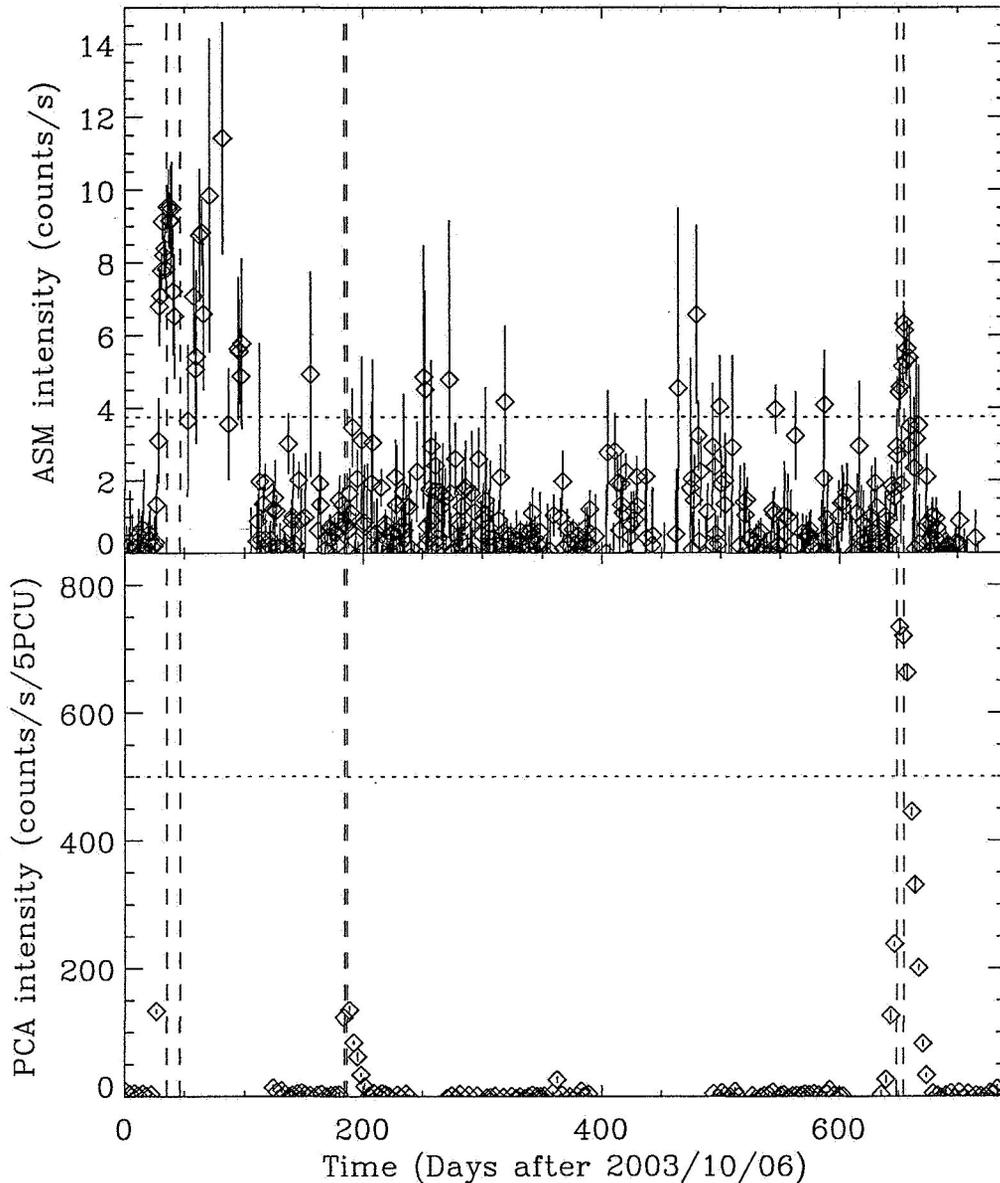
Fig. 1.— The long term ASM and PCA (galactic bulge scan) light curves of A1744–361. The pairs of dashed vertical lines show the time intervals of pointed *RXTE* observations of the source during the outbursts in 2003, 2004 and 2005. Each of these intervals contains several observations. The dotted horizontal lines give the 50 mCrab intensity level. Note that the PCA galactic bulge scan was prevented due to the angular proximity to the sun during the first outburst, which caused a data gap. We also note that during the years 1998 – 2002, the PCA galactic bulge scan did not find any outburst from A1744–361, which shows that this source exhibits an outburst rarely. The very low source luminosity during the quiescent state indicates that A1744–361 is a weak LMXB.
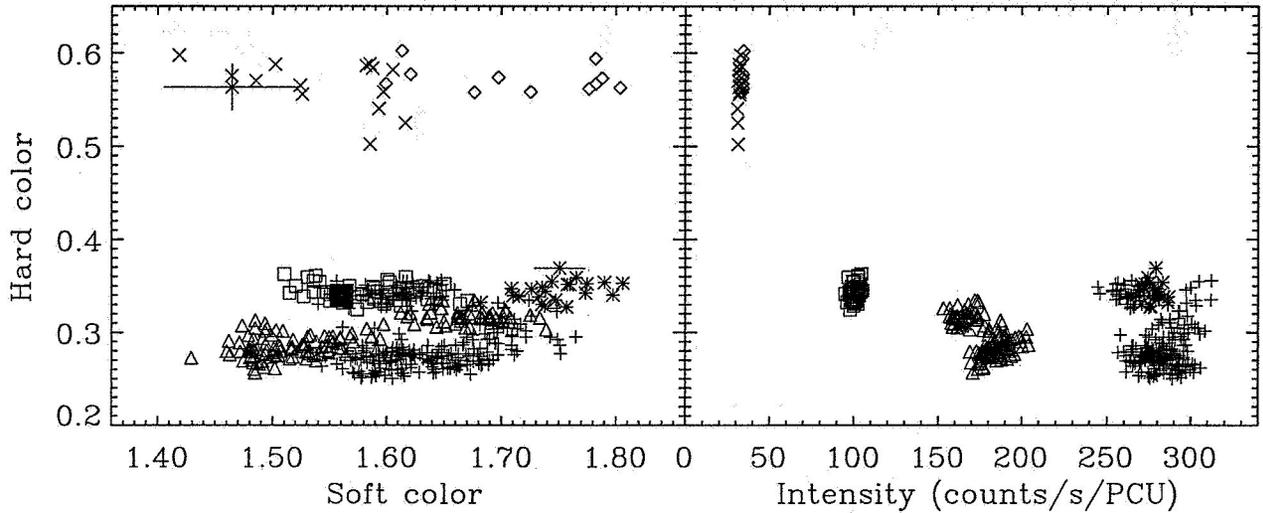
Fig. 2.— Color-color diagram (left panel) and hardness-intensity diagram (right panel) of A1744–361 using the *RXTE* PCA pointed observation data of the years 2003, 2004 and 2005. The definitions of the colors and the energy range of the intensity are given in § 2. Here we use the data only from the top Xenon layers. Each point is for 64 s of data. The *cross* symbols are for the ObsID 90058-04-02-00 (2004 data that show a ∼ 2.5 Hz QPO, and a possible kHz QPO (Bhattacharyya et al. 2006)), the *diamond* symbols are for ObsID 90058-04-01-00 (2004 data that show a ∼ 3.5 Hz QPO (Bhattacharyya et al. 2006)), the *square* symbols are for the ObsID 91050-05-01-00 (2005 data that show a thermonuclear X–ray burst (Bhattacharyya et al. 2006)), the *triangle* symbols are for the rest of the 2005 data, the *star* symbols are for the two segments of the ObsID 80431-01-02-00 (2003 data that show energy dependent dips (Bhattacharyya et al. 2006); but the dip portions are excluded), and the *plus* symbols are for the rest of the 2003 data. The *filled square* symbol is for the data just before the burst. Here we exclude the time intervals of obvious flares, burst and dips. Two sets (one for low intensity data and another for high intensity data) of typical 1σ error bars are shown in the color-color diagram. The ranges of soft color, hard color and intensity strongly indicate the atoll nature of A1744–361 during the outbursts (see § 2).
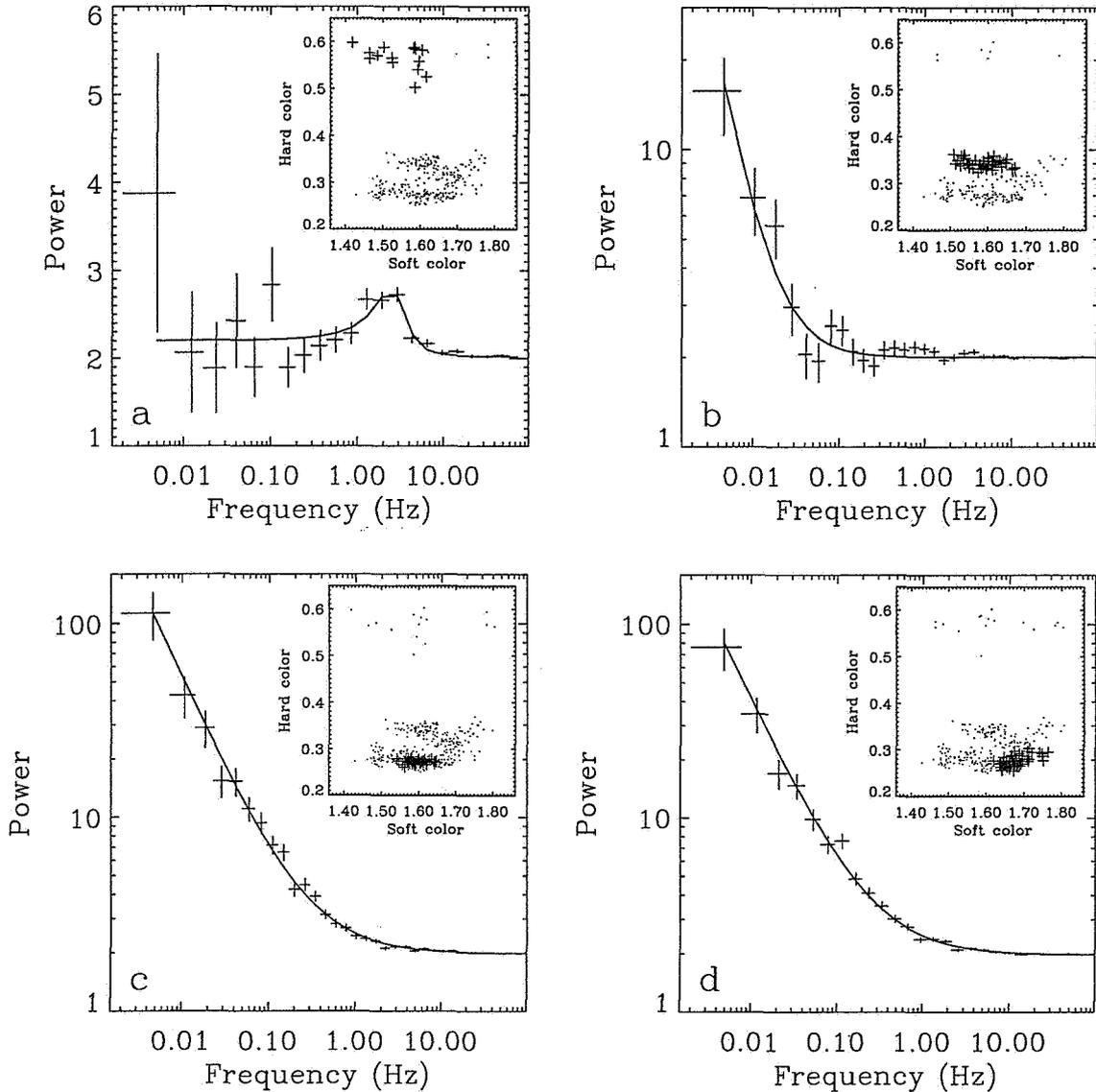
Fig. 3.— Low frequency power spectra (for the energy range ∼ 2.6 − 30 keV) of A1744–361 using *RXTE* PCA data. Panels *a*, *b*, *c* and *d* are for the ObsIDs 90058-04-02-00, 91050-05-01-00, 80431-01-02-04 and 80431-01-02-02 respectively. For each panel, the main panel shows the data points and the best fit model (solid line; see Table 1). The horizontal lines around the data points give the frequency bin, and the corresponding vertical lines give the 1σ errors of powers. Each inset panel shows the color-color diagram (same as in Fig. 2) and the *plus* symbols show the data used to calculate the power spectrum in the corresponding main panel. Panel *a* is for the low intensity AHB (see § 2) state of the source, and the power spectrum is well fitted with a constant+Lorentzian model. The 'constant' describes the Poisson noise level and the Lorentzian describes the dipper QPO (Bhattacharyya et al. 2006). Panels *b*, *c* and *d* are for the banana state of A1744–361, and a constant+powerlaw model fits the power spectra well. Here the 'powerlaw' describes the very low frequency noise (VLFN).
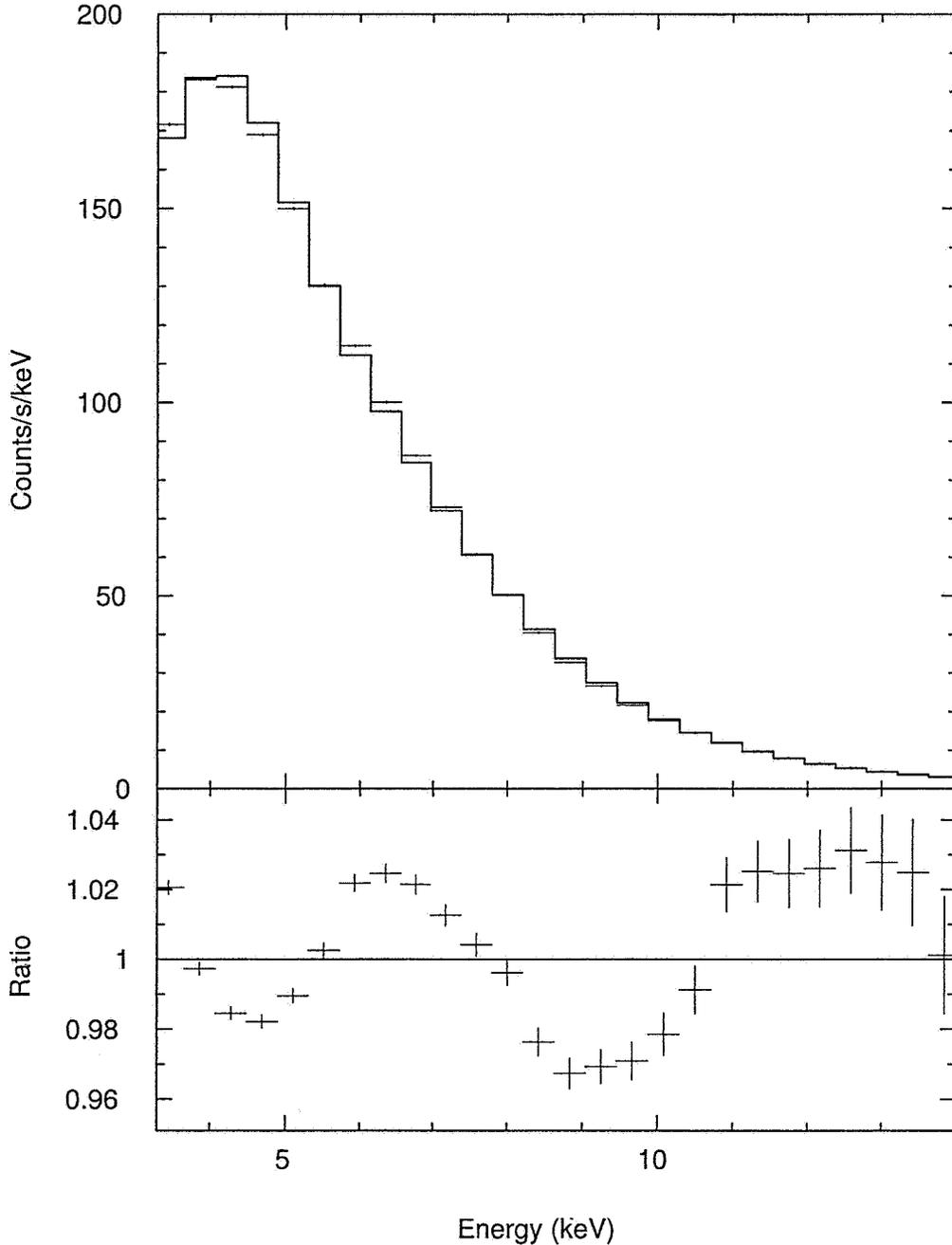
Fig. 4.— *RXTE* PCA energy spectrum from A1744–361 for the ObsID 80431-01-02-02 (time segment denoted by *plus* symbols of panel *d* of Fig. 3; high intensity banana state). Here we use only the top Xenon layers, and fit the data with a continuum model (*'ridge'+wabs*(compST+bbodyrad)* in *XSPEC*; model no. 2 of Table 3). The *'ridge'* model is the best fit model (*wabs*(raymond+powerlaw)* in *XSPEC*) for galactic ridge emission and we fix the parameters of this model to the best fit value (Table 2). The upper panel shows the data points and the model (solid histogram). The lower panel shows the data to model ratio. The lower panel suggests that an additional broad emission line model component (near $\sim$ 6 keV) and an additional absorption edge model component (near $\sim$ 8 keV) are required for a good fit.